Free Radical Biology & Medicine 47 (2009) 1753–1761

Contents lists available at ScienceDirect

Free Radical Biology & Medicine

journal homepage: www.elsevier.com/locate/freeradbiomed

Original Contribution

Fibroblasts from long-lived mutant mice show diminished ERK1/2 phosphorylation but exaggerated induction of immediate early genes

Liou Y. Sun [a], Michael J. Steinbaugh [a], Michal M. Masternak [b], Andrzej Bartke [b], Richard A. Miller [a,c,*]

[a] Department of Pathology and Geriatrics Center, University of Michigan, Ann Arbor, MI 48109, USA
[b] Department of Internal Medicine and Department of Physiology, Southern Illinois University School of Medicine, Springfield, IL 62794, USA
[c] Ann Arbor VA Medical Center, Ann Arbor, MI 48105, USA

ARTICLE INFO

Article history:
Received 31 July 2009
Revised 18 September 2009
Accepted 22 September 2009
Available online 26 September 2009

Keywords:
Aging
ERK
Fibroblast
Hydrogen peroxide
Longevity
Stress resistance
Snell dwarf mice
Free radicals

ABSTRACT

Skin-derived fibroblasts from long-lived mutant mice, including the Snell dwarf mice and mice defective in growth hormone receptor (GHRKO mice), are resistant to death induced by oxidative stress or by UV light, but the molecular mechanism for their stress resistance is unknown. This study shows that phosphorylation of the stress-activated protein kinases ERK1/2 induced by peroxide, cadmium, or paraquat is attenuated in cells from these mice. Induction of ERK phosphorylation by UV light was not altered in the Snell dwarf cells, and neither JNK nor p38 kinase showed increased phosphorylation in response to any of the stresses tested. Surprisingly, stress-induced elevation of mRNA for certain immediate early genes (Egr-1 and Fos) was higher in Snell-derived cells than in control cells, despite the evidence of lower ERK phosphorylation. Thus cells from Snell dwarf mice differ from controls in two ways: (a) lower induction of ERK1/2 phosphorylation and (b) increased expression of some ERK-dependent immediate early genes. These alterations in kinase pathways may contribute to the resistance of these cells to lethal injury.

Loss-of-function mutations at the Prop1 (Ames dwarf) and Pit1 (Snell dwarf) loci, as well as targeted disruption of the growth hormone receptor/binding protein gene, delay aging and greatly prolong life span in the mouse. The Ames and Snell dwarf mouse models are the best-studied mutants in which altered growth hormone (GH)/(insulin-life growth factor 1 (IGF-I) signals produce dramatic increases in life span with concomitant delay of late life diseases and disabilities [1,2]. Moreover, a number of aging-related phenotypes are also delayed in these mice, including collagen cross-linking, cataracts, kidney diseases, and fatal neoplastic disease, as well as declines in immune function, locomotor activity, learning, and memory [2–4]. The recessive mutation of either Prop1 or Pit1 genes leads to abnormal development of the anterior pituitary and thus to primary decline in production of GH, thyrotropin, and prolactin, with consequent declines in levels of circulating IGF-I and thyroxin. GH receptor/GH-binding protein knockout (GHRKO) mice were developed by targeted disruption of the Ghr/Ghrbp gene [5]. These mutant mice do not express the GH receptor, are GH resistant, and have profoundly suppressed circulating levels of IGF-I and insulin, markedly increased life span, and multiple indices of delayed aging [5–7].

Close association of enhanced stress resistance with extended longevity is well documented in lower species, including worms, flies, and yeast [8–10]. Our group has previously reported that skin-derived fibroblast cell lines from adult mice of the Ames, Snell, and GHRKO stocks, for example, are resistant to cell death induced by exposure to oxidative (H_2O_2, paraquat), nonoxidative (UV, and methyl methanesulfonate, or MMS), and mixed (heat, cadmium) stresses [11,12]. Fibroblasts from two other long-lived mouse mutants, i.e., the IGF-IR knockout and the p66shc splice variant, are also resistant to oxidative stress in vitro [13,14]. Fibroblasts from long-lived species also show unusually high resistance to multiple forms of lethal injury [15,16]. However, the molecular basis of the cellular stress resistance remains to be discovered.

The mitogen-activated protein kinases (MAPKs) comprise a ubiquitous group of signaling proteins that play a prominent role in regulating cell proliferation, differentiation, and adaptation. Members of each major MAPK subfamily, the extracellular signal-regulated protein kinases (ERK), the c-Jun N-terminal kinases (JNK), and p38 MAPK, have been implicated in cell injury and disease [17,18]. The MAPK signaling module is defined by a three-tiered kinase cascade, resulting in phosphorylation of a conserved Thr-X-Tyr activation motif by an upstream dual-specificity MAPK kinase [17]. In particular, ERK1 and ERK2, which are activated by the MAPK/ERK kinase-1/2 (MEK1/2), are emerging as important regulators of cellular responses to various stimuli [19].

The goal of this research project was to test the hypothesis that the high stress resistance of cells from Snell dwarf and GHRKO mice was related to unusually fast or strong signals mediated by one or more members of the MAPK family.

* Corresponding author. Fax: +1 734 647 9749.
E-mail address: millerr@umich.edu (R.A. Miller).

0891-5849/$ – see front matter © 2009 Elsevier Inc. All rights reserved.
doi:10.1016/j.freeradbiomed.2009.09.021

Materials and methods

Animals

Snell dwarf (homozygous dw/dw) animals (and heterozygote controls) were bred at the University of Michigan as the progeny of (DW/J×C3H/HeJ) dw/+ females and (DW/J×C3H/HeJ) F1 dw/dw males. The sires of the test mice had been treated with GH and thyroxin to increase body size and fertility. Littermates with the (+/dw) genotype were used as controls. Tail skin biopsies were taken from male mice 3–4 months of age. Protocols were approved by the University Committee on the Use and Care of Animals. GHRKO mice and littermate controls were generated at Southern Illinois University (Springfield, IL, USA), from breeding stock originally generated by Dr. John Kopchick's group at Ohio University. Tail skin biopsies from these mice were obtained from 3- to 6-month-old males and sent overnight on ice to the University of Michigan in Dulbecco's modified Eagle's medium (DMEM) supplemented with 20% heat-inactivated fetal calf serum (FCS), antibiotics, Fungizone, and 10 mM Hepes. Fibroblasts were prepared from the biopsy tissue as described [11]. GHRKO mice and normal littermate controls were produced by mating heterozygous (+/−) carriers of the disrupted Ghr/Ghbp gene or homozygous knockout (−/−) males with (+/−) females. The genetic background of these GHRKO animals is derived from 129/Ola embryonic stem cells and from BALB/c, C57BL/6, and C3H inbred strains [2].

Cell culture and treatment

Fibroblast cultures from all biopsies were isolated as previously reported [11]: tail skin biopsies were minced using a scalpel and then placed into a 35-mm dish with 1.5 ml of complete medium (DMEM, 10% FCS, 100 U ml^{-1} penicillin, 100 U ml^{-1} streptomycin, and 0.25 μg ml^{-1} Fungizone) and 1 ml of collagenase solution (1000 U ml^{-1}) in a humidified CO_2 incubator at 37°C containing room air with 20% O_2. After 24 h the cells were pipetted vigorously to separate the cells, passed through netting to remove large particles, and centrifuged for 5 min at 200 g. The cell pellet was resuspended in 3 ml of complete medium, transferred to a 25-cm^2 flask, and cultured to 90% confluence. At this point 0.75×10^6 cells were subcultured into 75-cm^2 flasks; this was considered passage 1. Each culture was passaged at 0.75×10^6 cells per 75-cm^2 flask every 4–6 days, depending on the experiment. On the second or third day after each subculturing two-thirds of the medium was replaced with fresh complete medium. Cell numbers were determined by hemacytometer. Each set of experiments made use of cells grown from three or four dw/dw mice and an equal number of littermate controls, with each cell line propagated and tested independently in parallel. Serum starvation was achieved by incubation in DMEM containing 2% bovine serum albumin (BSA) for at least 12 h before the direct addition of H_2O_2, paraquat (methyl viologen), or cadmium (Sigma) to this culture medium, after which cells were harvested at various times, as indicated, for biochemical assays. All measurements of stress-induced enzyme activity and gene expression were obtained from cells at passage 3.

Antibodies

Antibodies for immunoblotting were obtained as follows: p38 MAPK, phospho-p38 MAPK (Thr180/Tyr182), ERK, phospho-ERK (Thr202/Tyr204), JNK, phospho-JNK (Thr183/Tyr185), phospho-Akt (Ser473), and Akt (Thr308) were from Cell Signaling Technology (Beverly, MA, USA); β-actin was from Sigma–Aldrich Corp. (St. Louis, MO, USA); and goat anti-rabbit and goat anti-mouse antibodies were from Santa Cruz Biotechnology (Santa Cruz, CA, USA). The following secondary antibodies from Jackson ImmunoResearch (West Grove, PA) were used: fluorescein isothiocyanate (FITC)-conjugated donkey–mouse IgG, FITC-conjugated donkey–rabbit IgG, Rhodamine Red-X-conjugated donkey–goat IgG, Rhodamine Red-X-conjugated donkey–mouse IgG, Rhodamine Red-X-conjugated donkey–rat IgG, or biotin-conjugated donkey–rat IgG.

Real-time RT-PCR

Quantitative real-time PCR was performed using a Rotor-Gene 3000 system (Corbett Research) with a QuantiTect SYBR green RT-PCR kit (Bio-Rad Laboratories, Hercules, CA, USA) as described [20]. In brief, cells were homogenized with RNA extraction buffer (Trizol reagent; Invitrogen Life Technologies, Carlsbad, CA, USA) to yield total RNA following the manufacturer's instructions. Total RNA was reverse transcribed with poly(dT) oligodeoxynucleotide and SuperScript II (Invitrogen Life Technologies), using the manufacturer's recommended conditions. After an initial denaturation step (95°C for 90 s), amplification was performed over 40–45 cycles of denaturation (95°C for 10 s), annealing (60°C for 5 s), and elongation (72°C for 13 s). Amplification was monitored by measuring the fluorimetric intensity of SYBR Green I at the end of each elongation phase. Glyceraldehyde-3-phosphate dehydrogenase (GAPDH) or β-actin expression was quantified to normalize the amount of cDNA in each sample. The change in threshold cycle number (ΔC_t) was normalized to the GAPDH reference gene by subtracting $\Delta C_{t\ GAPDH}$ from $\Delta C_{t\ gene}$. The effect of treatment ($\Delta\Delta C_t$) was calculated by subtracting $\Delta C_{t\ normal}$ from $\Delta C_{t\ Tg}$. Fold induction was determined by calculating $2^{\Delta\Delta Ct}$.

Western blot analysis

After exposure to various forms of stress, cells were washed in ice-cold phosphate-buffered saline (PBS) and then harvested in 1 ml of lysis buffer [20 mM Tris (pH 7.5), 150 mM NaCl, 1% Triton X-100, with protease inhibitor cocktail and phosphatase inhibitor cocktails (Sigma–Aldrich Corp.)] and spun at 12,000 rpm for 40 min. The supernatants were removed and stored at −70°C. Protein concentrations were determined using the bicinchoninic acid assay (Pierce Corp., Rockford, IL, USA) according to the manufacturer's instructions. For Western blotting, protein extracts were mixed with sample buffer (Bio-Rad) and boiled for 5 min. Forty micrograms of total protein was separated electrophoretically according to size by SDS–PAGE using Criterion XT Precast Gel (Bio-Rad) for 60 min at 150 V. Proteins were then wet-transferred for 1 h at 100 V onto nitrocellulose membranes. Membranes were rinsed briefly in Tris-buffered saline (TBS; pH 7.6) and blocked with 5% dry milk (or 3% BSA for phosphorylated proteins) in TBS plus 0.05% Tween 20 (TBST) for 1 h at room temperature. Blots were washed with TBST and incubated with the primary antibody diluted in the appropriate blocking solution at 4°C overnight with shaking. After incubation, blots were washed three times (15 min each) with TBST and incubated with an appropriate secondary antibody. For visualization of specific bands in the chemiluminescence assays, the membrane was exposed to X-OMAT film; for chemifluorescence the membrane was incubated with enhanced chemifluorescence substrate and a digital image was generated with the Molecular Dynamics (Sunnyvale, CA, USA) Storm system. Quantification of immunoblot signals was performed using the ImageQuant software package (Molecular Dynamics).

Immunofluorescence imaging

Fibroblasts were seeded at 5000 cells per well and grown to subconfluence on eight-well LabTek II chamber glass slides. Staining was performed under baseline conditions and after overnight serum starvation followed by stress stimulation. Cells were washed in PBS and fixed in ice-cold methanol for 10 min at −20°C. After being blocked with 20% normal goat serum in PBS for 1 h at room temperature, the cells were incubated with the primary antibody overnight at 4°C. The cells were washed in PBS and incubated with fluorescent goat anti-mouse or

goat anti-rabbit IgG for 1 h at room temperature. After the cells were washed again in PBS, the nuclei were stained with DAPI, and the slides were mounted with Vectashield (Vector Laboratories). Negative controls were processed in a similar fashion, except incubation with the primary antibody was omitted. Cells were imaged using a confocal fluorescence microscope (Olympus IX SLA). Images were then imported into Adobe Photoshop (Adobe Systems) for processing. Fluorescence mounting medium was applied before the coverslips were placed onto the slides. Quantification of immunoreactive cells was performed following a reported procedure [21] with image analyzer software (Image-Pro Plus; Media Cybernetics).

Statistical analyses

All bar graphics show mean values ± SEM. Differences between normal and dwarf cells in the levels of protein phosphorylation were evaluated using a paired t-test, with each time point considered separately, using $p = 0.05$ as the criterion for significance. Data for induction of intermediate early gene expression were evaluated by analysis of variance (factors: genotype and treatment), followed by planned comparisons of peroxide vs. no treatment, peroxide vs peroxide with ERK inhibitor, and dwarf vs control cells for each exposure condition.

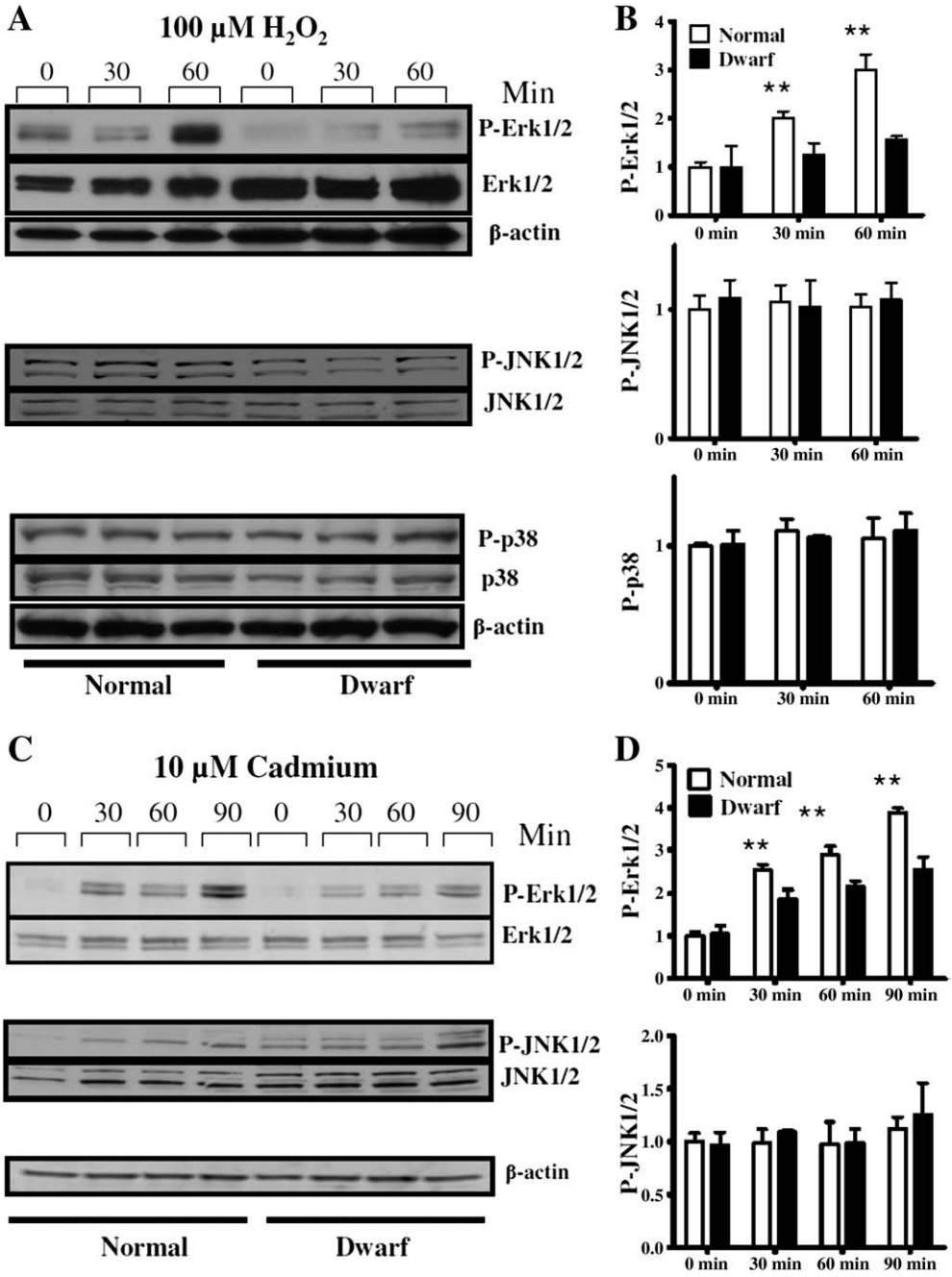

Fig. 1. Phosphorylation of ERK1/2, JNK1/2, and p38 in skin-derived primary fibroblasts from Snell dwarf and normal mice in response to (A and B) H_2O_2 and (C and D) cadmium. After serum starvation for 12–24 h, cells were treated with H_2O_2 (100 μM, equivalent to 600 nmol of H_2O_2 per million cells) or cadmium (10 μM) for the indicated periods and then stained for p-ERK1/2, p-JNK1/2, or p-p38. (A and C) Representative autoradiographs of Western blots for phosphorylated and total forms of ERK1/2, JNK1/2 and p38 protein in dwarf and control cells. (B and D) The means and SEM ($N = 6$ pairs of dwarf and control mice), as ratios to unstressed control cells at 0 min. $^{**}p < 0.01$.

Results

Phosphorylation of MAPKs in skin-derived primary fibroblasts from Snell dwarf mice in response to multiple stresses

We speculated that differential activation of MAPK family members may contribute to the molecular mechanisms that confer resistance to stress in fibroblasts from long-lived Snell dwarf mice. We examined the levels of the phosphorylation of various members of the MAPK family by Western blotting. As shown in Fig. 1A, we found that low doses of H_2O_2 led to significant increases in phosphorylation of ERK1/2 in both Snell dwarf cells and control cells. Interestingly, the phosphorylation of ERK1/2 by H_2O_2 was dramatically attenuated in dwarf fibroblasts compared with normal fibroblasts (Fig. 1). By 60 min, phosphorylation levels had increased in control cells by approximately threefold, compared to a 50% increase in the dwarf cells. In contrast, phosphorylation of JNK1/2 or p38 was not increased by H_2O_2 exposure, and there was no difference between dwarf and control cells in the level of phosphorylation of JNK1/2 or p38 before or after exposure to H_2O_2. The graphic shows means and standard error of the mean for $N=6$ pairs of mice, expressed as a ratio to the level of p-ERK1/2 measured in normal cells not exposed to H_2O_2. The differences between dwarf and control cells at 30 and 60 min are significant at $p<0.01$.

We also tested the activation of MAPK pathways by other stressors including paraquat and cadmium. Consistent with the data on H_2O_2 exposure, paraquat and cadmium both induced phosphorylation of ERK1/2, which was significantly attenuated in dwarf cells compared with control cells (Figs. 1 and 2). JNK phosphorylation was not sensitive to cadmium or paraquat treatment in cells from mutant or control mice.

We also evaluated the effects of UV light on the phosphorylation of ERK1/2 and JNK1/2. Cells were exposed to 40 mJ/cm^2 UV irradiation and harvested at various times after treatment. As shown in Figs. 2C

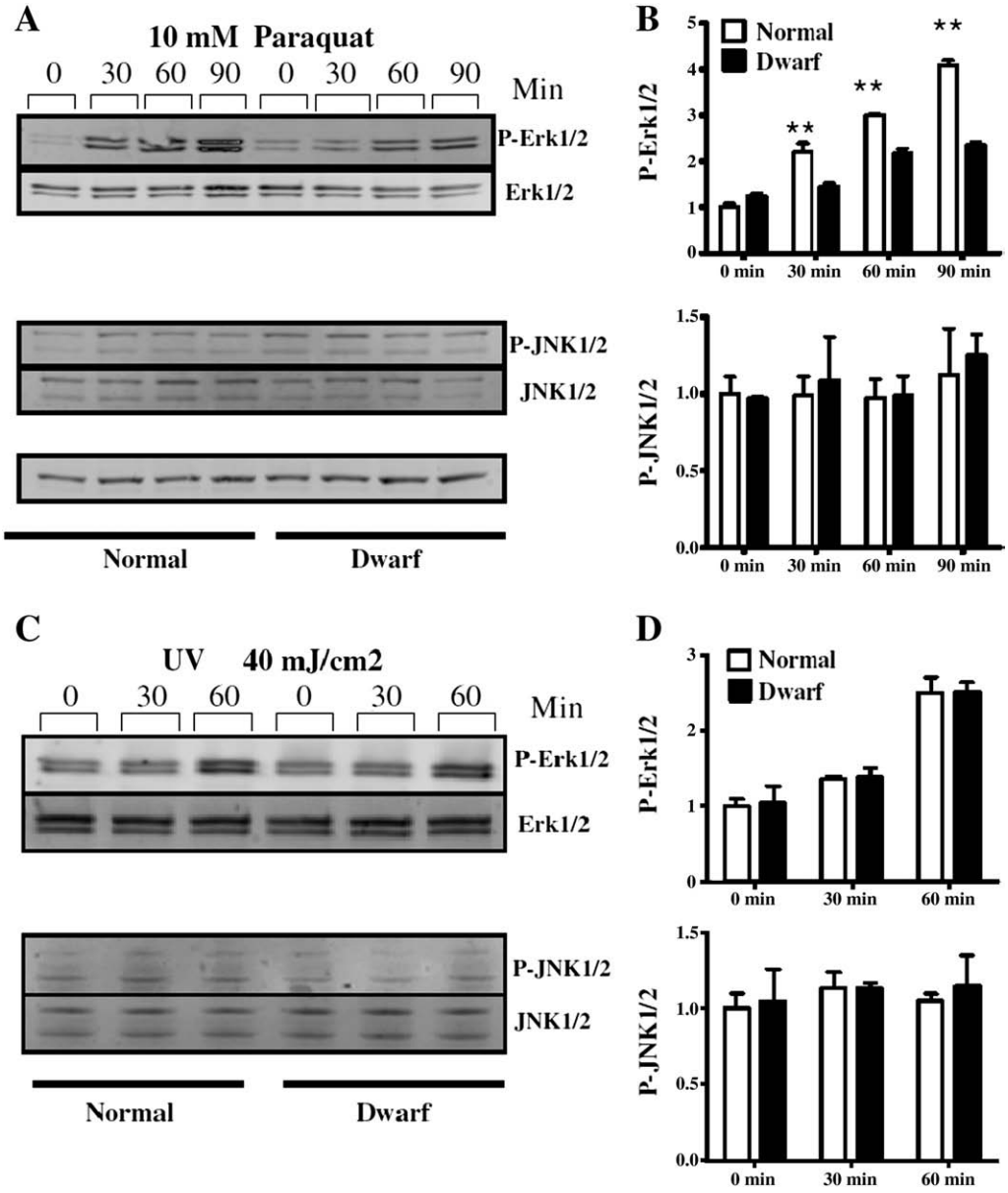

Fig. 2. Phosphorylation of ERK1/2 and JNK1/2 in skin-derived primary fibroblasts from Snell dwarf and normal mice in response to (A and B) paraquat and (C and D) UV light. After serum starvation for at least 12–24 h, cells were treated with paraquat (10 mM) for the indicated periods or exposed to UV light (40 mJ/cm^2) and further incubated for the time indicated. (A and C) Representative autoradiographs of Western blots for phosphorylated and total forms of ERK1/2and JNK1/2 protein, in dwarf and control cells. (B and D) The means and SEM ($N=6$ pairs), as ratios to unstressed control cells at 0 min. **$p<0.01$.

and D, UV induced a modest increase in ERK1/2 phosphorylation in both dwarf and normal cells, but this did not differ between the genotypes, and no significant phosphorylation of JNK1/2 could be observed in either dwarf or normal cells.

Differences (between dwarf and normal cells) in phosphorylation of ERK1/2 in response to H_2O_2 stimulation were confirmed by an immunofluorescence study (Fig. 3) using an antibody specific for phosphorylated ERK1/2. p-ERK1/2 signals were distributed throughout the cytoplasm and nucleus, with considerably higher fluorescence intensities in normal cells compared with dwarf cells after exposure to H_2O_2. The response in the normal cells was approximately two- to threefold higher than the response in the dwarf cells evaluated in parallel. These results are in good agreement with the immunoblotting experiments illustrated in Fig. 1.

Increased H_2O_2-induced expression of ERK-dependent early growth response genes in cells from Snell dwarf mice

The early growth response gene (Egr-1) encodes a zinc-finger-containing DNA-binding protein, and levels of Egr-1 mRNA rise very rapidly in response to various forms of stress [22]. It has been shown recently that the increase in expression of Egr-1 is important for the resistance of cells to apoptotic stimuli [23]. We therefore investigated whether dwarf and normal cells differ in the expression

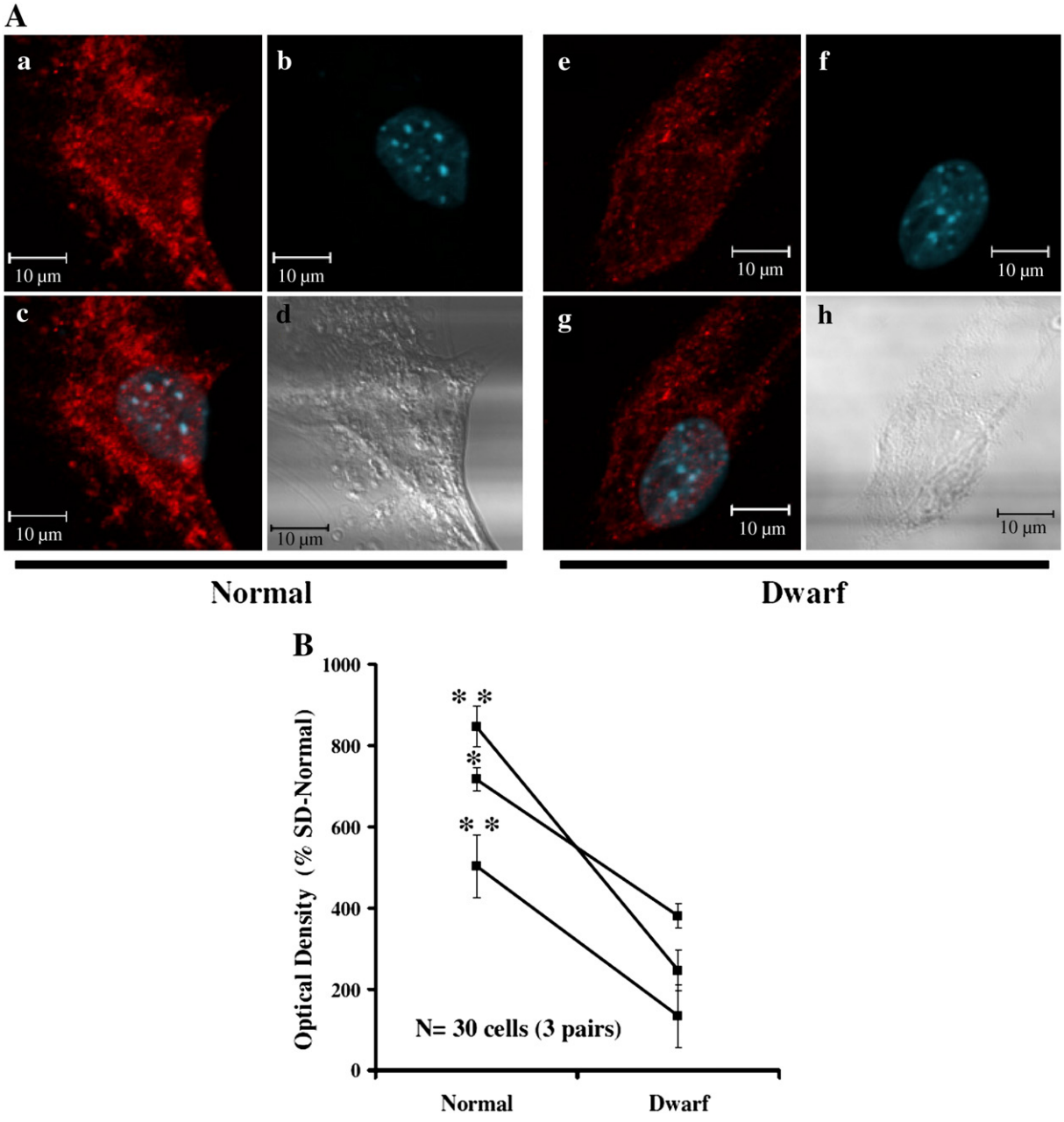

Fig. 3. Immunohistochemical detection of H_2O_2-induced ERK1/2 phosphorylation in fibroblasts from normal and dwarf mice. (A) Each set of four images shows representative confocal images of a cell treated with H_2O_2 (100 μM for 60 min) from a normal or a dwarf mouse. Cells were labeled for phosphorylation of ERK1/2 (red; a and e) or DAPI staining (blue; b and f). The merged images show both DAPI and p-ERK1/2 (c and g). DIC images of the cells are shown in the lower right panels (d and h). Scale bar, 10 μm. (B) Relative fluorescence intensities for three dwarf and three normal mice (10 cells from each of the six mice). Only cells giving fluorescence above a threshold determined from the control section (using Image-Pro Plus software) were counted. *$p<0.05$; **$p<0.01$. Control experiments to measure nonspecific binding to tissue sections were performed by incubation in buffer overnight without the primary antibody.

of this transcription factor in response to H_2O_2 exposure. Total mRNA prepared from cells exposed to 100 μM H_2O_2 for 1 h was subjected to Q-RT-PCR analysis. As shown in Fig. 4A, Egr-1 mRNA levels were robustly up-regulated in both normal and dwarf cells after H_2O_2 treatment. Surprisingly, the Egr-1 response of dwarf cells to this oxidative stress was much stronger than the response of control cells. The increase in the Egr-1 gene expression induced by H_2O_2 was potently inhibited by exposure to PD98059, an inhibitor of MEK (a MAPK kinase), added before the H_2O_2 stress (Fig. 4A). The results of this experiment indicate that ERK activation by MEK is required, in both normal and dwarf cells, for the induction of Egr-1 expression by H_2O_2. The inhibitory effect of PD98059 on peroxide-induced Egr-1 expression was at least as strong in cells from dwarf mice as in cells from normal mice. A similar pattern was seen for mRNA levels of another immediate early gene, Fos (Fig. 4): dramatic stimulation by H_2O_2 in dwarf compared to control cells and attenuation by the MEK inhibitor. Peroxide-induced stimulation of Jun mRNA was less intense than the induction of Egr-1 and Fos, but showed a similar pattern. Fig. 4 also shows mRNA levels for Gapdh, a peroxide-insensitive negative control. These results suggest that up-regulation of Egr-1, Fos, and Jun mRNA is mediated at least partially by ERK signals and is substantially stronger in dwarf than in control fibroblasts.

Skin-derived primary fibroblasts from GHRKO mice also show diminished ERK phosphorylation in response to H_2O_2 and paraquat

Mice with a targeted disruption in the growth hormone receptor/GH-binding protein (GHRKO) have profoundly suppressed circulating levels of IGF-I and insulin, markedly increased life span, and multiple indices of delayed aging [6]. Previously, we have reported that fibroblasts from GHRKO mice were also resistant to death induced by H_2O_2, UV light, and paraquat compared to fibroblasts from littermate control mice [12]. To see if the defects in ERK1/2 phosphorylation noted in fibroblasts from Snell dwarf mice were also characteristic of GHRKO fibroblasts, we evaluated phosphorylation of several MAPK enzymes in these cells. We found that 100 μM H_2O_2 and 10 mM paraquat rapidly induced phosphorylation of ERK1/2, but not of JNK or p38 kinases, in GHRKO and control cells (Fig. 5). Similar to the results from cells from Snell dwarf mice, stress-induced ERK1/2 activation was significantly attenuated in GHRKO cells compared with control cells (Fig. 5). Despite the diminution of H_2O_2-mediated ERK1/2 phosphorylation, induction of transcription of Egr-1 and Fos mRNA was elevated in GHRKO compared to control fibroblasts (Fig. 6), consistent with the results seen in cells from Snell dwarf mice. Induction of Jun mRNA was equivalent in cells from both mutant and control mice.

The superoxide dismutase (SOD) family of enzymes, which catalyze the dismutation of superoxide into H_2O_2 and oxygen, is thought to help defend against oxidative damage that might contribute to age-related pathology and cellular dysfunction. Many cell lines are highly dependent on SOD for survival and are sensitive to its suppression [24]. We found higher levels of Sod2 and Sod3 mRNA in GHRKO cell lines compared to controls. There was no alteration in transcription level of these two mRNAs after H_2O_2 stimulation (Fig. 7) in control or mutant cells. These data support the idea that increased SOD expression might contribute to the resistance of GHRKO cells to death after oxidant treatment in vitro.

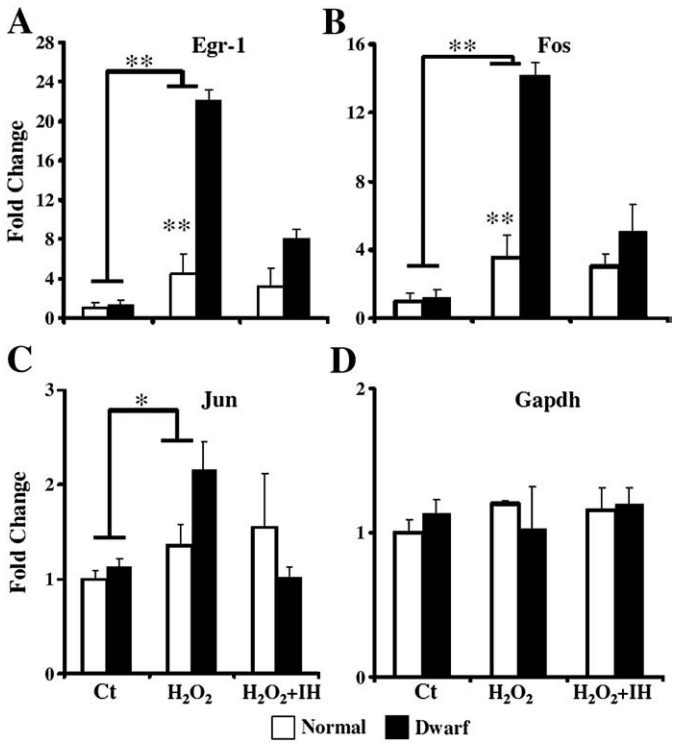

Fig. 4. Expression of (A) Egr-1, (B) Fos, and (C) Jun mRNA levels in cultured Snell and control fibroblasts with or without exposure to H_2O_2. mRNA was measured using real-time RT-PCR after 60 min of 100 μM H_2O_2 stimulation in the presence or absence of the MEK inhibitor (IH) PD98059 (50 μM). Data were normalized to Gapdh values (D) and expressed as fold change of cDNA in dwarf cells relative to control (normal cells without any treatment). Each bar represents the mean ± SEM of six pairs of dwarf and normal donors. (*$p<0.05$; **$p<0.01$). Control (Ct) cells were incubated in serum-free medium without H_2O_2.

Discussion

This study shows that phosphorylation of the stress-activated ERK1/2 kinases induced by peroxide, cadmium, or paraquat was attenuated in cells from long-lived Snell dwarf mice. The Snell-derived cells did not differ from controls in ERK phosphorylation after UV treatment, and JNK and p38 did not show increased phosphorylation in response to any of the stresses tested in these cells. Immunofluorescence analysis of single cells showed that the attenuation of ERK1/2 phosphorylation in cells from dwarf mice represented a change in most of the cells in the cultures, rather than a change in the proportion of responsive to unresponsive cells. Paradoxically, the stress-induced elevation of mRNA of Egr-1 and Fos, members of the immediate early gene family, was higher in Snell dwarf cells than in control cells. Cells from long-lived GHRKO mice were, like Snell dwarf cells, relatively unresponsive to peroxide- and paraquat-mediated stimulation of ERK1/2 phosphorylation and also hypersensitive in tests for Egr-1 and Fos gene expression. The disparity between the findings of ERK1/2 phosphorylation (lower in cells from mutant mice) and those for ERK-dependent gene activity (elevated in mutant-derived cells) could not be attributed to some ERK-independent signal pathway, because the increase in Egr-1 and Fos gene expression induced by peroxide was almost completely blunted by a MEK inhibitor.

These results have several implications concerning the mechanism of resistance, in GHRKO and Snell dwarf-derived skin fibroblasts, to lethal injury. It is not well understood how agents like cadmium, peroxide, and paraquat activate MEK and ERK, and it seems likely that the steps in these injury-responsive pathways may differ from agent to agent. Paraquat, for example, augments oxidative damage from free radicals produced, gradually, by intracellular mitochondria, whereas peroxide is likely to cause injury more rapidly by reactions with cellular membranes. The diminution of ERK1/2 phosphorylation (and thus presumably of MEK activity) in cells from Snell and GHRKO mice thus suggests that fibroblasts from the long-lived mutants are less susceptible to early steps in one or more of these damage-detection pathways. It is possible, for example, that the damage initiated by

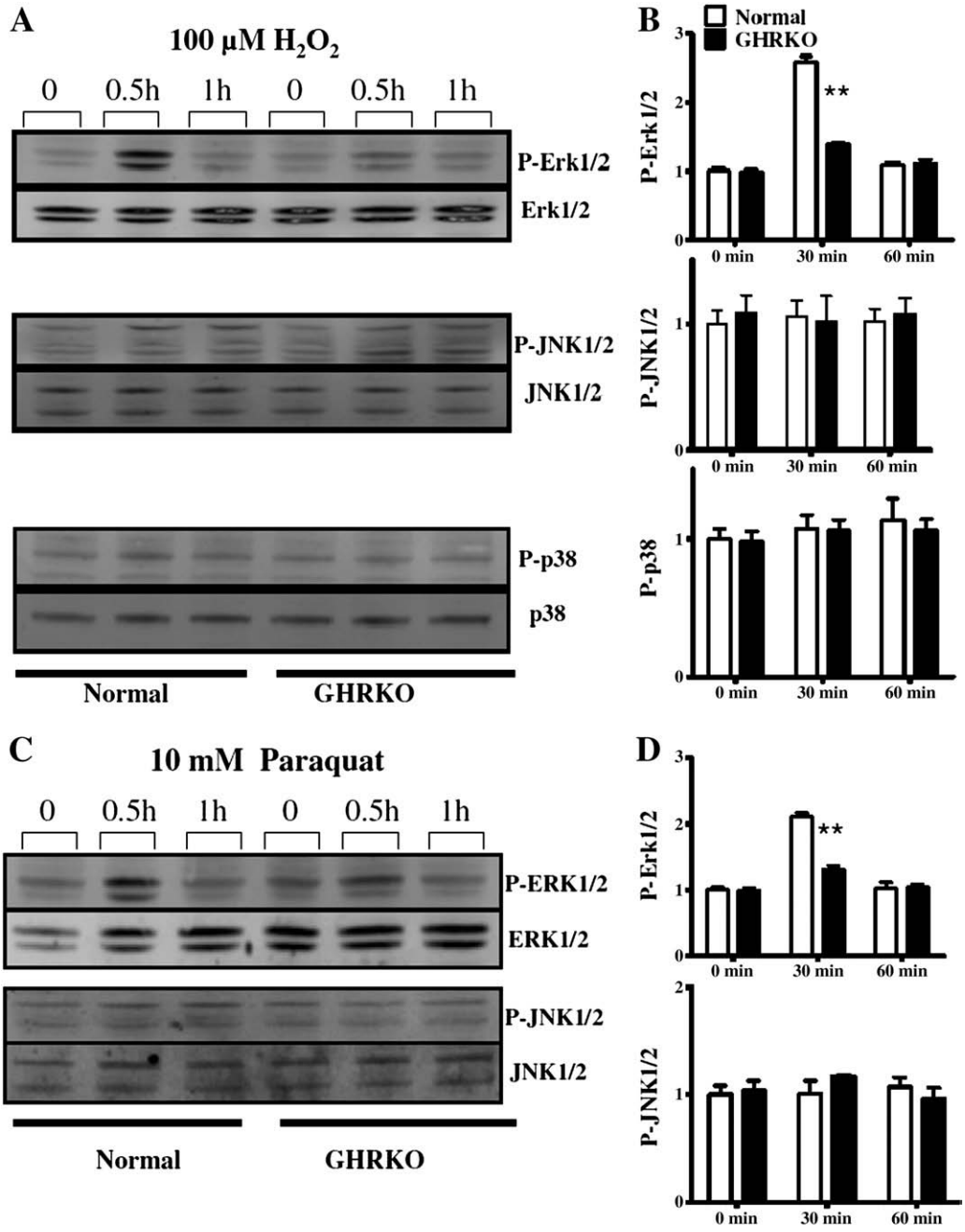

Fig. 5. Phosphorylation of ERK1/2, JNK1/2, and p38 signaling in skin-derived primary fibroblasts from GHRKO and normal mice in response to (A and B) H_2O_2 and (C and D) paraquat. (A and C) Representative autoradiographs of Western blots for phosphorylated and total forms of ERK1/2, JNK1/2, and p38 proteins in GHRKO and control cells after treatment. (B and D) Phosphorylated/total ERK1/2, JNK, and p38 as ratios to unstressed control cells. Means ± SEM are shown ($N = 5$ pairs; $^{**}p < 0.01$).

H_2O_2 in cellular membranes might be repaired more quickly in Snell cells than in control cells, thus blunting the MEK-induction signal at an early stage. Experiments that evaluate the earliest stages of damage induction, and that evaluate stages in the kinase cascade upstream from MEK, will be needed to address these ideas.

Despite the lower levels of stress-induced ERK1/2 phosphorylation, cells from the long-lived mutant mice show higher levels of mRNA production from at least two of the immediate early genes, i.e., Egr-1 and Fos. This surprising result suggests strongly that some of the immediate early genes are hyperresponsive to even blunted signals from ERK activation. Further work comparing these cells for cofactors that modulate transcription of immediate early genes as well as the maturation and stability of their mRNAs may be rewarding. It is plausible, though not at all certain, that improved activation of immediate early genes may contribute to the resistance of dwarf-derived fibroblasts to lethal injury in vitro.

The extracellular signal-regulated protein kinases are integrally involved in regulating pivotal processes, including proliferation, differentiation, adaptation (i.e., cell motility, long-term potentiation), survival, and cell death. The ERK signaling module involves sequential activation of Raf (MAPKKK), MEK1/2 (MAPKK), and ERK1/2 (MAPK) [17,19]. ERK1/2 is crucial for resistance to oxidative stress, and the cascade is known to be activated by oxidative injury [25–27]. Hydrogen peroxide stimulates extracellular signal-regulated protein kinases in pulmonary arterial smooth muscle cells [27], but these kinases can exhibit dual effects on cell death depending on the

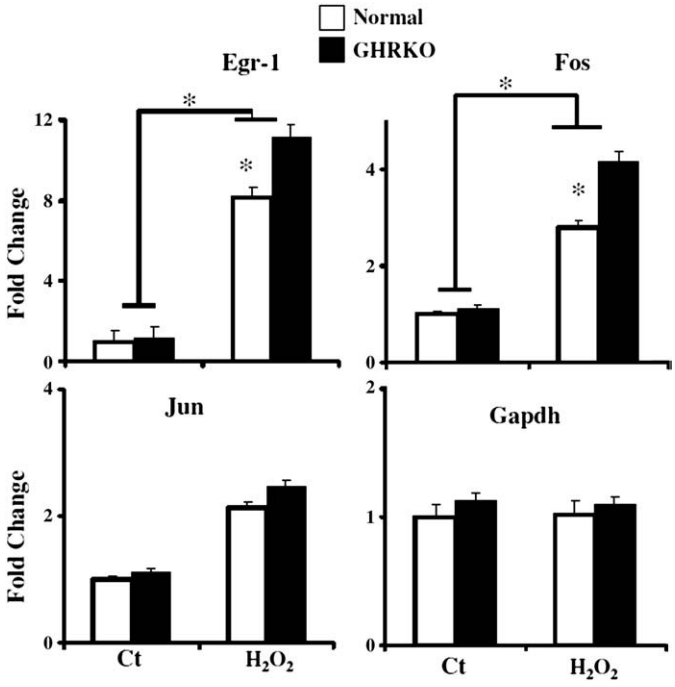

Fig. 6. Expression of Egr-1, Fos, and Jun mRNA in GHRKO and control fibroblasts with or without 30 min exposure to 100 μM H_2O_2. Data were normalized to Gapdh values and expressed as fold change of cDNA in GHRKO cells relative to unstressed control cells. Each bar shows the mean ± SEM of five pairs of dwarf and mutant donors (*$p<0.05$).

kinetics, duration, intensity, and context of activation [28]. ERK activation has been shown to promote cell survival under some conditions [29,30], but it increases the sensitivity to oxidative stress under other conditions [31]. Inhibition of ERK abrogates cell death induced by H_2O_2 in pancreatic cancer cells [32] and protects against glutamate-induced neuronal death [33]. In the present context, it is noteworthy that fibroblasts from Snell dwarf mice, though resistant to many forms of lethal injury [11,12], are actually more susceptible than control cells to the lethal effects of agents (tunicamycin and thapsigargin) that induce apoptosis through the ER (endoplasmic reticulum) stress pathway [34]. Whether the diminished levels of ERK phosphorylation or the hypersensitivity of ERK-responsive mRNAs contributes to these cells' sensitivity to ER stress deserves further exploration.

These biochemical abnormalities add to the growing list of properties that distinguish control fibroblasts from those of Snell dwarf mice. In addition to differences in responses to lethal stresses, Snell dwarf cells also show resistance to inhibition of the plasma membrane redox system induced either by low doses of rotenone or by culture in very low glucose concentrations [35]. They are also relatively resistant to the growth crisis induced when primary mouse fibroblasts are cultured in 20% oxygen and have faster growth rates and higher levels of cell accumulation in long-term cultures compared to control cells [36]. Repair of UV-induced DNA damage, with restoration of RNA transcription, is also accelerated in cells from Snell dwarf animals [37]. It is not yet understood how these many cellular properties are coordinately induced, during early life development, in the skin tissue of GHRKO and Snell dwarf mice, nor is it understood how the properties are maintained, in vitro, during many rounds of replication under standardized growth conditions. The rationale for detailed analysis of the properties of fibroblasts derived from these long-lived mice depends on the assumption that similar traits may also arise, in vivo, in cell types that play a more prominent role in disease susceptibility and tissue maintenance. The association between whole-organism longevity, differences in insulin/IGF-I intracellular signals, and resistance to multiple forms of lethal stress was first noted in *Caenorhabditis elegans* [8] and has also been demonstrated in *Drosophila melanogaster* [9], suggesting that this set of coordinated responses evolved at an early stage of metazoan diversity, a stage predating the splitting of nematode, arthropod, and vertebrate lineages.

The elucidation of differences in fibroblasts from long-lived and control mice should help us to devise strategies for testing related hypotheses about stress resistance pathways in multiple cell types in vivo. Our findings would predict, for example, that some cell types of long-lived mice are likely to show both diminished ERK phosphorylation and exaggerated responses of ERK-dependent genes, when exposed to stresses like those used in our in vitro work. A recent study, for example, shows that inhibition of Ras/ERK1/2 signaling is associated with resistance to oxidative damage of rat cortical neurons in vitro [38]. ERK signaling has also been suggested to be involved in neurodegeneration [28,39]. For example, in Parkinson's disease (PD), ERK is activated after application of the toxin 6-hydroxydopamine. Under these conditions, cell death is decreased by PD98059, an inhibitor of ERK activation [40]. Activated ERK is also found in Lewy bodies, pathological hallmarks of PD that consist of aggregated α-synuclein in the degenerated neurons from PD patients [41]. It should be rewarding to explore protocols in which Snell dwarf and control mice are compared for resistance to various forms of in vivo injury and to agents that induce varying forms of degenerative or neoplastic disease, to see if the long-lived mice are resistant and, if so, to determine if alterations in ERK-dependent signals play a role in the altered disease susceptibility.

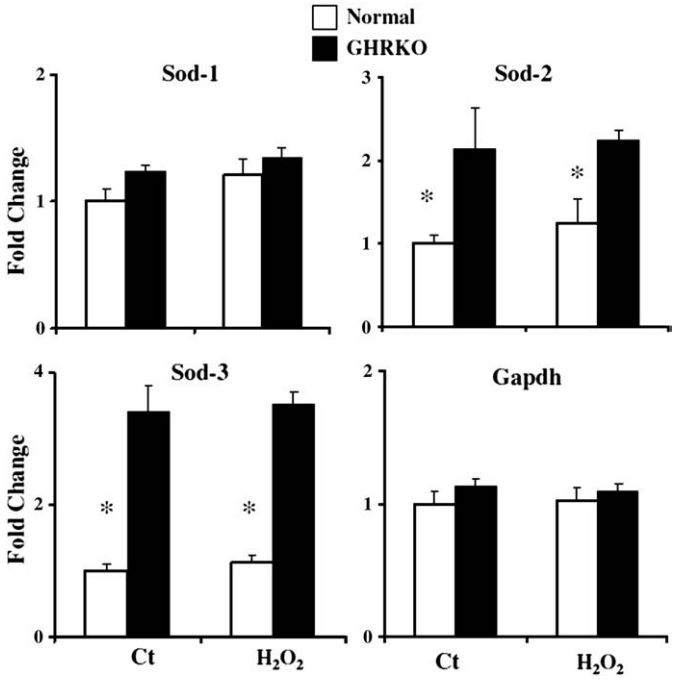

Fig. 7. Expression of Sod mRNAs in fibroblasts from GHRKO mice with or without 30 min exposure to 100 μM H_2O_2. Data were normalized to Gapdh values and expressed as fold change of cDNA in GHRKO cells relative to unstressed control cells. Each bar shows the mean ± SEM of five pairs of mutant and normal donors (*$p<0.05$).

Acknowledgments

This work was supported by NIH Grants AG023122, U19 AG023122, and AG019899. We thank John Kopchick for the gift of breeding pairs for the GHRKO mouse stock. We thank Maggie Lauderdale, William Kohler, and Lisa Burmeister for technical assistance.

References

[1] Brown-Borg, H. M.; Borg, K. E.; Meliska, C. J.; Bartke, A. Dwarf mice and the ageing process. *Nature* **384:**33; 1996.

[2] Flurkey, K.; Papaconstantinou, J.; Miller, R. A.; Harrison, D. E. Lifespan extension and delayed immune and collagen aging in mutant mice with defects in growth hormone production. *Proc. Natl. Acad. Sci. USA* **98:**6736–6741; 2001.

[3] Ikeno, Y.; Bronson, R. T.; Hubbard, G. B.; Lee, S.; Bartke, A. Delayed occurrence of fatal neoplastic diseases in Ames dwarf mice: correlation to extended longevity. *J. Gerontol. A Biol. Sci. Med. Sci.* **58:**291–296; 2003.

[4] Kinney, B. A.; Meliska, C. J.; Steger, R. W.; Bartke, A. Evidence that Ames dwarf mice age differently from their normal siblings in behavioral and learning and memory parameters. *Horm. Behav.* **39:**277–284; 2001.

[5] Zhou, Y.; Xu, B. C.; Maheshwari, H. G.; He, L.; Reed, M.; Lozykowski, M.; Okada, S.; Cataldo, L.; Coschigamo, K.; Wagner, T. E.; Baumann, G.; Kopchick, J. J. A mammalian model for Laron syndrome produced by targeted disruption of the mouse growth hormone receptor/binding protein gene (the Laron mouse). *Proc. Natl. Acad. Sci. USA* **94:**13215–13220; 1997.

[6] Bartke, A. Role of the growth hormone/insulin-like growth factor system in mammalian aging. *Endocrinology* **146:**3718–3723; 2005.

[7] Bonkowski, M. S.; Rocha, J. S.; Masternak, M. M.; Al Regaiey, K. A.; Bartke, A. Targeted disruption of growth hormone receptor interferes with the beneficial actions of calorie restriction. *Proc. Natl. Acad. Sci. USA* **103:**7901–7905; 2006.

[8] Larsen, P. L. Aging and resistance to oxidative damage in Caenorhabditis elegans. *Proc. Natl. Acad. Sci. USA* **90:**8905–8909; 1993.

[9] Lin, Y. J.; Seroude, L.; Benzer, S. Extended life-span and stress resistance in the Drosophila mutant methuselah. *Science* **282:**943–946; 1998.

[10] Martin, G. M.; Austad, S. N.; Johnson, T. E. Genetic analysis of ageing: role of oxidative damage and environmental stresses. *Nat. Genet.* **13:**25–34; 1996.

[11] Murakami, S.; Salmon, A.; Miller, R. A. Multiplex stress resistance in cells from long-lived dwarf mice. *FASEB J.* **17:**1565–1566; 2003.

[12] Salmon, A. B.; Murakami, S.; Bartke, A.; Kopchick, J.; Yasumura, K.; Miller, R. A. Fibroblast cell lines from young adult mice of long-lived mutant strains are resistant to multiple forms of stress. *Am. J. Physiol. Endocrinol. Metab.* **289:**E23–29; 2005.

[13] Holzenberger, M.; Dupont, J.; Ducos, B.; Leneuve, P.; Geloen, A.; Even, P. C.; Cervera, P.; Le Bouc, Y. IGF-1 receptor regulates lifespan and resistance to oxidative stress in mice. *Nature* **421:**182–187; 2003.

[14] Migliaccio, E.; Giorgio, M.; Mele, S.; Pelicci, G.; Reboldi, P.; Pandolfi, P. P.; Lanfrancone, L.; Pelicci, P. G. The p66shc adaptor protein controls oxidative stress response and life span in mammals. *Nature* **402:**309–313; 1999.

[15] Harper, J. M.; Salmon, A. B.; Leiser, S. F.; Galecki, A. T.; Miller, R. A. Skin-derived fibroblasts from long-lived species are resistant to some, but not all, lethal stresses and to the mitochondrial inhibitor rotenone. *Aging Cell* **6:**1–13; 2007.

[16] Kapahi, P.; Boulton, M. E.; Kirkwood, T. B. Positive correlation between mammalian life span and cellular resistance to stress. *Free Radic. Biol. Med.* **26:** 495–500; 1999.

[17] Chang, L.; Karin, M. Mammalian MAP kinase signalling cascades. *Nature* **410:** 37–40; 2001.

[18] Junttila, M. R.; Li, S. P.; Westermarck, J. Phosphatase-mediated crosstalk between MAPK signaling pathways in the regulation of cell survival. *FASEB J.* **22:**954–965; 2008.

[19] Roux, P. P.; Blenis, J. ERK and p38 MAPK-activated protein kinases: a family of protein kinases with diverse biological functions. *Microbiol. Mol. Biol. Rev.* **68:** 320–344; 2004.

[20] Sun, L. Y.; D'Ercole, A. J. Insulin-like growth factor-I stimulates histone H3 and H4 acetylation in the brain in vivo. *Endocrinology* **147:**5480–5490; 2006.

[21] Brami-Cherrier, K.; Valjent, E.; Herve, D.; Darragh, J.; Corvol, J. C.; Pages, C.; Arthur, S. J.; Girault, J. A.; Caboche, J. Parsing molecular and behavioral effects of cocaine in mitogen- and stress-activated protein kinase-1-deficient mice. *J. Neurosci.* **25:** 11444–11454; 2005.

[22] Thiel, G.; Cibelli, G. Regulation of life and death by the zinc finger transcription factor Egr-1. *J. Cell. Physiol.* **193:**287–292; 2002.

[23] Pipaon, C.; Casado, J. A.; Bueren, J. A.; Fernandez-Luna, J. L. Jun N-terminal kinase activity and early growth-response factor-1 gene expression are down-regulated in Fanconi anemia group A lymphoblasts. *Blood* **103:**128–132; 2004.

[24] Huang, P.; Feng, L.; Oldham, E. A.; Keating, M. J.; Plunkett, W. Superoxide dismutase as a target for the selective killing of cancer cells. *Nature* **407:**390–395; 2000.

[25] Gaitanaki, C.; Konstantina, S.; Chrysa, S.; Beis, I. Oxidative stress stimulates multiple MAPK signalling pathways and phosphorylation of the small HSP27 in the perfused amphibian heart. *J. Exp. Biol.* **206:**2759–2769; 2003.

[26] Guyton, K. Z.; Liu, Y.; Gorospe, M.; Xu, Q.; Holbrook, N. J. Activation of mitogen-activated protein kinase by H_2O_2: role in cell survival following oxidant injury. *J. Biol. Chem.* **271:**4138–4142; 1996.

[27] Zhang, J.; Jin, N.; Liu, Y.; Rhoades, R. A. Hydrogen peroxide stimulates extracellular signal-regulated protein kinases in pulmonary arterial smooth muscle cells. *Am. J. Respir. Cell Mol. Biol.* **19:**324–332; 1998.

[28] Chu, C. T.; Levinthal, D. J.; Kulich, S. M.; Chalovich, E. M.; DeFranco, D. B. Oxidative neuronal injury: the dark side of ERK1/2. *Eur. J. Biochem.* **271:**2060–2066; 2004.

[29] Johnson, G. L.; Lapadat, R. Mitogen-activated protein kinase pathways mediated by ERK, JNK, and p38 protein kinases. *Science* **298:**1911–1912; 2002.

[30] Wada, T.; Penninger, J. M. Mitogen-activated protein kinases in apoptosis regulation. *Oncogene* **23:**2838–2849; 2004.

[31] Subramaniam, S.; Zirrgiebel, U. von Bohlen und Halbach, O.; Strelau, J.; Laliberte, C.; Kaplan, D. R.; Unsicker, K. ERK activation promotes neuronal degeneration predominantly through plasma membrane damage and independently of caspase-3. *J. Cell Biol.* **165:**357–369; 2004.

[32] Osada, S.; Sakashita, F.; Hosono, Y.; Nonaka, K.; Tokuyama, Y.; Tanaka, H.; Sasaki, Y.; Tomita, H.; Komori, S.; Matsui, S.; Takahashi, T. Extracellular signal-regulated kinase phosphorylation due to menadione-induced arylation mediates growth inhibition of pancreas cancer cells. *Cancer Chemother. Pharmacol.* **62:**315–320; 2008.

[33] Satoh, T.; Nakatsuka, D.; Watanabe, Y.; Nagata, I.; Kikuchi, H.; Namura, S. Neuroprotection by MAPK/ERK kinase inhibition with U0126 against oxidative stress in a mouse neuronal cell line and rat primary cultured cortical neurons. *Neurosci. Lett.* **288:**163–166; 2000.

[34] Salmon, A. B.; Sadighi Akha, A. A.; Buffenstein, R.; Miller, R. A. Fibroblasts from naked mole-rats are resistant to multiple forms of cell injury, but sensitive to peroxide, ultraviolet light, and endoplasmic reticulum stress. *J. Gerontol. A Biol. Sci. Med. Sci.* **63:**232–241; 2008.

[35] Leiser, S. F.; Salmon, A. B.; Miller, R. A. Correlated resistance to glucose deprivation and cytotoxic agents in fibroblast cell lines from long-lived pituitary dwarf mice. *Mech. Ageing Dev.* **127:**821–829; 2006.

[36] Maynard, S. P.; Miller, R. A. Fibroblasts from long-lived Snell dwarf mice are resistant to oxygen-induced in vitro growth arrest. *Aging Cell* **5:**89–96; 2006.

[37] Salmon, A. B.; Ljungman, M.; Miller, R. A. Cells from long-lived mutant mice exhibit enhanced repair of ultraviolet lesions. *J. Gerontol. A Biol. Sci. Med. Sci.* **63:** 219–231; 2008.

[38] Li, Y.; Xu, W.; McBurney, M. W.; Longo, V. D. SirT1 inhibition reduces IGF-I/IRS-2/Ras/ERK1/2 signaling and protects neurons. *Cell Metab.* **8:**38–48; 2008.

[39] Irving, E. A.; Bamford, M. Role of mitogen- and stress-activated kinases in ischemic injury. *J. Cereb. Blood Flow Metab.* **22:**631–647; 2002.

[40] Kulich, S. M.; Chu, C. T. Sustained extracellular signal-regulated kinase activation by 6-hydroxydopamine: implications for Parkinson's disease. *J. Neurochem.* **77:** 1058–1066; 2001.

[41] Zhu, J. H.; Kulich, S. M.; Oury, T. D.; Chu, C. T. Cytoplasmic aggregates of phosphorylated extracellular signal-regulated protein kinases in Lewy body diseases. *Am. J. Pathol.* **161:**2087–2098; 2002.